REVIEW

A review of heat transfer data for single circular jet impingement

K. Jambunathan, E. Lai, M. A. Moss* and B. L. Button
Department of Mechanical Engineering, Nottingham Polytechnic, Nottingham, UK

Experimental data for the rate of heat transfer from impinging turbulent jets with nozzle exit Reynolds numbers in the range of 5,000–124,000 have been collated and critically reviewed from the considerable body of literature available on the subject. The geometry considered is that of a single circular jet impinging orthogonally onto a plane surface for nozzle-to-plate distances from 1.2–16 nozzle diameters and over a flow region up to six nozzle diameters from the stagnation point. Existing correlations for local heat transfer coefficient express Nusselt number as a function of nozzle exit Reynolds number raised to a constant exponent. However, the available empirical data suggest that this exponent should be a function of nozzle-to-plate spacing and of the radial displacement from the stagnation point. A correlation for Nusselt number of the form suggested by this evidence has been derived using a selection of the data. The review also suggests that the Nusselt number is independent of nozzle-to-plate spacing up to a value of 12 nozzle diameters at radii greater than six nozzle diameters from the stagnation point. The results from a simple extrapolation for obtaining heat transfer coefficients in the wall jet region compare favourably with published data.

Keywords: jet impingement; forced convection correlation; turbulent flow

Introduction

Impinging jets are widely used where high rates of heat transfer are desired. To improve the design of these systems a knowledge of the parameters affecting the heat transfer rate is required.

The heat transfer rate to or from a jet impinging onto a surface is a complex function of many parameters: Nusselt number (Nu), Reynolds number (Re), Prandtl number (Pr), the nondimensional nozzle-to-plate spacing (z/D), and the nondimensional displacement from the stagnation point (x/D). In addition, the effects of nozzle geometry, flow confinement, turbulence, recovery factor, and dissipation of jet temperature have all been shown to be significant. A selection of publications that consider the effect of these parameters on the heat transfer rate and empirical investigations into the flow phenomena in an impinging jet are reviewed.

The work of Martin (1977), Obot *et al.* (1979a), and Goldstein and Franchett (1988) among others has resulted in the establishment of empirical correlations for evaluating either local or area mean heat transfer. These correlations do not take account of an expected radial variation in the effect of Reynolds number, which is expected to occur as the flow and thermal boundary layers develop.

In many cases the heat transfer data presented only extends a few nozzle diameters from the stagnation point. A means of extrapolating data to give heat transfer rates in the wall jet is required.

*Present address: Rolls-Royce plc, Derby, UK.
Address reprint requests to Dr. Jambunathan at the Department of Mechanical Engineering, Nottingham Polytechnic, Nottingham, NG1 4BU, UK.

Received 20 August 1990; accepted 27 January 1992

A literature review of single circular jet impingement heat transfer

Jet flow characteristics

The flow in an air jet impinging orthogonally on a plane surface is commonly divided into four zones (Figure 1):

(1) There is a developing flow zone where fluid from the surroundings is entrained into the jet, thus reducing the jet velocity. This mixing or shear region surrounds a core where the fluid velocity at the nozzle centerline (U_m) is almost equal to the nozzle exit velocity (U_n). The core region is often referred to as the potential core even though the flow is not inviscid. A common definition of the end of the core region is the point where $U_m = 0.95U_n$. A core length of six nozzle diameters has been suggested by Gautner *et al.* (1970) based on a survey that covered a large range of turbulent Reynolds numbers.

(2) At greater nozzle-to-plate spacings the axial velocities reduce with increasing distance from the nozzle exit. An analysis by Schlichting (1968) showed that the fall of the centerline velocity and the jet half width (width of the jet where $U = U_m/2$) will be directly proportional to the axial distance from the end of the potential core.

(3) The region near the impingement plate is often referred to as the deflection zone where there is a rapid decrease in axial velocity and a corresponding rise in static pressure. The measurements of Tani and Komatsu (1966) showed that this zone extends approximately two nozzle diameters from the plate surface. Giralt *et al.* (1977) proposed a value of $1.2D$ for the height of the deflection zone.

(4) Within the wall jet the transverse velocity profile shows

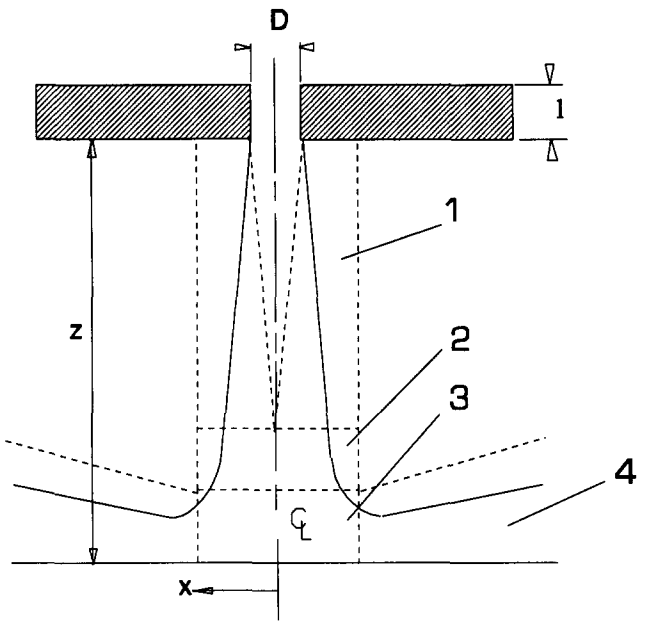

Figure 1 Flow zones in an impinging jet. Zone 1, initial mixing region; zone 2, established jet; zone 3, deflection zone; zone 4, wall jet

that the local velocity rises rapidly to a maximum near to the wall and then falls at greater distances from the wall. The wall jet exhibits higher levels of heat transfer than parallel flow. This appears to be due to turbulence generated by the shear between the wall jet and the ambient air, which is transported to the boundary layer at the heat transfer surface.

Heat transfer characteristics

An analytical solution for heat transfer at a stagnation point in a laminar flow (Sibulkin 1952) shows that

$$Nu \propto U_m^{1/2}$$

suggesting that the Nusselt number should remain roughly

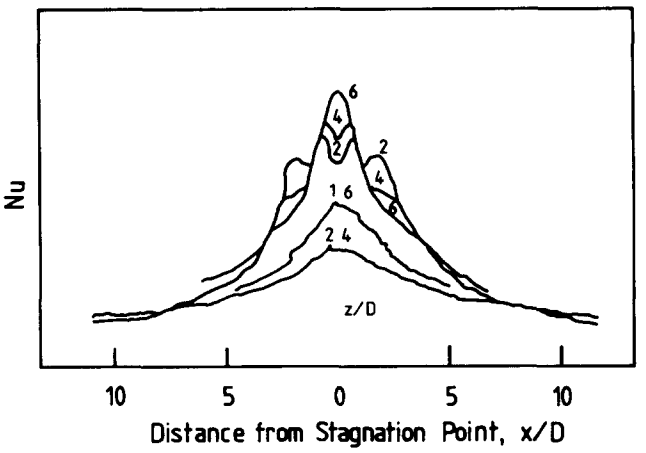

Figure 2 Radial variation of heat transfer coefficient between a plate and an impinging jet. (Data from Gardon and Carbonpue 1962)

constant in the core region and reduce downstream of the core.

The axial variations of velocity and turbulence for slot jets issuing into an unconfined environment were investigated by Gardon and Akfirat (1965). Their results showed that the turbulence intensity in a free jet could reach 30 percent of nozzle exit velocity at approximately eight nozzle diameters downstream of the nozzle. The axial distance from the nozzle at which the maximum turbulence intensity occurs appears to coincide with that of the maximum stagnation point heat transfer. Measurements using circular nozzles have also given similar results; e.g., Schlunder and Gnielinski (1967) found both the maximum turbulence and the maximum stagnation point heat transfer occurring at $z/D = 7.5$. Gardon and Akfirat suggested that the increasing level of turbulence causes the heat transfer rate at the stagnation point to increase even beyond the end of the potential core where the jet centerline velocity is falling. The increase in heat transfer rate ceases when the increase in turbulence does not compensate for the fall in the jet velocity.

The radial variation of heat transfer coefficients measured by Gardon and Corbonpue (1962) are given in Figure 2. These curves show local maxima in the heat transfer rate at the lower

Notation

a	Constant
Cp	Specific heat, w/Kg K
D	Nozzle exit diameter, m
D_{AB}	Diffusion coefficient, m^2/s
h	Heat transfer coefficient, w/m^2 K
k	Coefficient
l	Nozzle length, m
Nu	hD/λ
Pr	Prandtl number
Pu	Potential core length, m
Q	Heat flux, w/m^2
Re	Reynolds number, $D\ U_n/v$
Sc	Schmidt number, $\mu/\rho D_{AB}$
Sh	Sherwood number, kD/D_{AB}
T	Temperature, K
t	Static temperature, K
Tu	Turbulence intensity, percentage main velocity component
U	Velocity, m/s
z	Axial distance nozzle to plate, m
x	Radial distance from stagnation point, m

Greek symbols

λ	Conductivity air, w/m K
μ	Viscosity, Ns/m^2
v	Kinematic viscosity, m^2/s
ρ	Density, kg/m^3

Subscripts

amb	Ambient
aw	Adiabatic wall
m	Centerline value
n	Nozzle exit
rec	Recovery
s	Stagnation point
w	Wall
1/2	Half width

values of nozzle-to-plate spacing ($z/D < 6$). For impinging circular jets at small z/D the heat transfer coefficient is seen to increase between the stagnation point and approximately $x/D = 0.5$. A second maximum is produced by circular jets at approximately $x/D = 2$. Gardon and Carbonpue also reported that at lower Reynolds numbers three maxima were visible at radial displacements of 0.5, 1.4, and 2.5 nozzle diameters from the stagnation point. As the Reynolds number was increased to approximately 20,000 the two outer maxima merged and only two maxima were seen. The presence of these three peaks in the radial distribution of heat transfer was confirmed by Popiel and Boguslawski (1988).

Three causes for the peaks in the radial distribution of heat transfer have been proposed:

The peak at $x/D = 0.5$ has been explained by the change in radial velocity, with displacement from the stagnation point. The radial velocity accelerates rapidly in the deflection region, but at greater radii the spreading of the jet causes the radial velocity to reduce.

Gardon and Akfirat (1965) suggested that the increase in heat transfer coefficient within the range $1 \leqslant x/D \leqslant 2$ can be explained by a transition from laminar to turbulent boundary-layer flow. At greater radial distances from the stagnation point a fall in the heat transfer rate occurs because of the fall in flow velocity in the radial direction. This mechanism will not apply to impinging jets that are fully developed or to impinging jets at large nozzle-to-plate spacings, which result in turbulent boundary-layer flow at the stagnation point. Velocity measurements (Launder 1991) in the boundary layer of an impinging jet for $z/D = 2$ show the presence of turbulence at the stagnation point.

The position of the maximum at $x/D = 2$ coincides approximately with the point where toroidal vortices, which form in the shear region around the circumference of the jet, strike the plate as highlighted in the flow visualization carried out by Popiel and Trass (1982) at $z/D = 1.2$ and 2. Popiel and Trass (1991) suggested that the vortices cause a pulsation in the jet that is responsible for the synchronized appearance of the next toroidal vortex around the entire nozzle circumference. They also show that ring-shaped eddies are formed in the wall jet at approximately the point where the toroidal vortices reach the plate.

Flow visualization photographs obtained by Yokobori *et al.* (1979) also show these toroidal vortices being convected to the impingement plate. These vortices coalesce, and for $z/D > 4$ the large-scale vortex structure appears to break down into small-scale random turbulence that penetrates to the jet axis. Radial movement of the stagnation point of the order of one nozzle diameter was also reported. However, a potential core exists for $z/D < 4$ where the vortices do not penetrate. The penetration of the vortices to the geometric stagnation point and the radial movement of the stagnation point help to break down any distinct flow regions. This may explain why the secondary maxima in the radial distribution of heat transfer coefficient become indistinct and the profiles begin to assume a bell shape for nozzle-to-plate spacings greater than $z/D = 4$.

The apparent disappearance of the large-scale vortex structure at larger nozzle-to-plate spacings is probably due to mixing of the smoke or dye used in these visualizations. Tso and Hussain (1989), using a grid of hot-wire anemometers, showed that ring, helical, and double helical vortex structures exist at large nozzle-to-plate spacings ($z/D = 50$). The helical structure was found to be dominant, this structure appeared to be responsible for significant entrainment of ambient air and jet spreading. The effects of vortices in the deflection zone near to the stagnation point have been detected by Kataoka *et al.* (1987, 1988) using a hot-wire anemometer. They showed a correlation between stagnation point Nusselt number and a "surface-renewal" parameter that is proportional to the frequency and magnitude of these vortices, the correlation was obtained for z/D between 2 and 10.

The flow visualizations of Popiel and Trass, Tso and Hussain, Yokobori *et al.*, and Kataoka *et al.* were conducted using jets issuing from elliptical or bell-shaped convergent nozzles. Popiel and Trass (1991) suggested that a laminar boundary layer formed in nozzles of these types is essential to the formation of a well-defined vortex structure. They gave results for a jet issuing from a nozzle that was designed to disrupt this laminar layer; the visualization shows a much less distinct vortex structure. This suggestion is supported by Lepicovsky (1989), who studied the effect of nozzle exit boundary-layer thickness on the length of the potential core. This study suggested that a thin laminar boundary layer at the nozzle exit resulted in higher rates of jet mixing than a thick boundary layer. However, turbulence measurements made by Yokobori *et al.* at the nozzle exit suggest that the vortex structure can still be obtained when the boundary layer at the nozzle exit is turbulent.

Causes of scatter in the experimental data

Nozzle geometry. Obot *et al.* (1979b, 1979c, 1982) suggested that the variations in turbulence levels due to different nozzle designs have brought about the variations in measured heat transfer rate, particularly in the optimal nozzle-to-plate spacing for maximum heat transfer. For a nozzle with a sharp-edged inlet and a length-to-diameter ratio of 1 (Re = 29,485) the maximum stagnation point Nusselt number, equal to 155, occurs at $z/D = 4$, and with a contoured inlet the maximum, Nu = 125, occurs at $z/D = 8$. The data given by Popiel and Boguslawski (1988) show that the area mean heat transfer due to an impinging jet issuing from a contoured ASME nozzle is 25 percent less than that of a jet from a sharp-edged orifice when $z/D = 4$, Re = 20,000, and $x/D = 1$. The effect of nozzle geometry on heat transfer is most significant in the region near the stagnation point. A similar investigation was made by Gundappa *et al.* (1989), who compared the axial velocity decay and the impingement heat transfer due to orifice jets and to jets issuing from pipes ($l/D = 10$). The axial velocity was seen to decay more slowly in the case of the jet produced by the pipe. Gundappa *et al.* suggested that this led to the higher values of Nusselt number seen for the impinging pipe jet at all radial positions when $z/D = 7.8$. At smaller nozzle-to-plate spacings the different nozzle designs were seen to produce differing shapes of radial Nusselt number distribution.

Nozzle geometry affects the velocity profile at the nozzle exit, which it has been suggested might be expected to affect the behavior of the toroidal vortices around the jet circumference and the turbulence level generated in the shear layer. The turbulence level would in turn affect the heat transfer coefficients. This turbulent behavior also affects the mixing of the jet with the ambient air and so the rate of velocity decay, which also influences the heat transfer coefficients.

Effect of small-scale turbulence. Den Ouden and Hoogendoorn (1974) and Hoogendoorn (1977), among others, have investigated the effect of small-scale turbulence on heat transfer in impinging jet systems. Hoogendoorn showed that the level of turbulence at the nozzle exit has an impact on the heat transfer at the stagnation point. For instance an increase in the axial turbulence intensity from 0.5–3.2 percent (at Re = 60,000 and $z/D = 2$) has resulted in an increase in the Nusselt number at the stagnation point from 180–215 and has eliminated the local minimum in heat transfer coefficient often

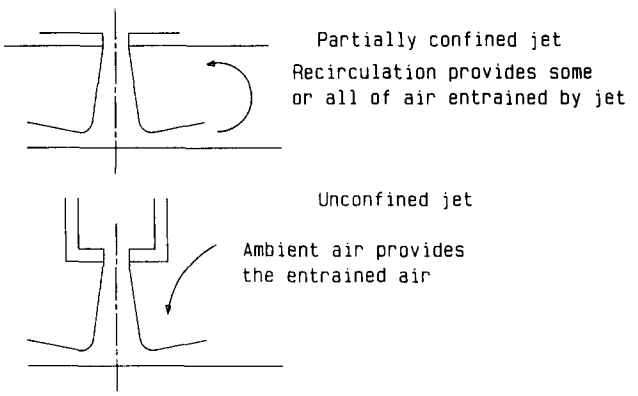

Figure 3 Schematic diagram of confined and unconfined jets

seen at small nozzle-to-plate spacings. However, the results of Gardon and Akfirat (1965) showed that the effect of nozzle exit turbulence on heat transfer is relatively small for $z/D > 6$ where turbulence generated in the shear layer predominates.

Confinement. Obot *et al.* (1982) showed that confinement (Figure 3) causes a reduction in the heat transfer rate. This reduction increases with increasing flow rate. At $z/D = 6$ and $x/D = 6$ a 4 percent reduction in the heat transfer due to flow confinement occurred at a Reynolds number of 29,673 and a reduction of 10 percent occurred at Re = 50,367. The data appears to show that this reduction will be least when $z/D = 6$.

The wall jet

Rao and Trass (1964) presented results that suggested that within the range $2.0 \leqslant z/D \leqslant 19.23$ the local mass transfer is independent of nozzle-to-plate spacing at radial positions greater than 4.5 nozzle diameters from the stagnation point. In addition they proposed an expression for Sherwood number, Sh, where

$$\mathrm{Sh} = 1.3\mathrm{Re}^{0.84}(x/D)^{-1.27}$$

Dawson and Trass (1966), by using a momentum integral analysis and assuming a 1/7th power law velocity profile between the wall and the point of maximum velocity in the wall jet, obtained an expression where the Sherwood number is independent of nozzle height:

$$\mathrm{Sh} = 0.0509\mathrm{Re}^{0.832}(x/D)^{-1}$$

This expression was obtained for unity Schmidt number (Sc); the exponents in this relationship are dependent on Schmidt number.

Mitachi and Ishiguro (1977) reported velocity and temperature measurements for a nozzle-to-plate spacing of less than one. They deduced two power laws: a value of between 1/10th to 1/14th for the velocity profile and 1/14th for the temperature profile. By assuming 1/14th power laws for the velocity and temperature profiles they demonstrated that

$$\mathrm{Nu} \propto \mathrm{Re}(x/D)^{-1.08}$$

Hrycak (1978) proposed the following expression based on the Colburn analogy and the wall shear stress derived by Poreh *et al.* (1967):

$$\overline{\mathrm{Nu}} = 1.95\mathrm{Pr}^{0.33}\mathrm{Re}^{0.7}(2x/D)^{-1.23}$$

Figure 4 shows the local heat transfer rate at $x/D = 6$ obtained from the papers summarized in Table 1. This plot supports the suggestion that, for z/D in the range of 2–12, the heat or mass transfer is independent of nozzle-to-plate spacing at sufficiently high radial displacements from the stagnation point. Figure 5 compares the radial distribution of heat transfer in the wall jet region obtained by Goldstein *et al.* (1986) and Hollworth and Gero (1985). It can be seen that for radii greater than about 4 nozzle diameters the local heat transfer is independent of the nozzle-to-plate spacing. Curves fitted to this data for $x/D \geqslant 4.5$ show

$$\mathrm{Nu} \propto (x/D)^{-a}$$

where $0.95 \leqslant a \leqslant 1.02$.

Using the assumption

$$\mathrm{Nu} \propto (x/D)^{-1}$$

based on the wall jet results it can be seen that $\overline{\mathrm{Nu}}/\mathrm{Pr}^{1/3}$ will approach zero asymptotically as x/D increases.

Effect of temperature recovery and of a nonambient jet

Studies were carried out by Hollworth and Wilson (1984) and Hollworth and Gero (1985) using jets heated up to 60°C above ambient temperature. These studies demonstrated that the Nusselt numbers derived using the adiabatic wall temperature are independent of the relative temperature. The adiabatic wall temperature was taken as the temperature that the heat transfer surface assumes when it is in equilibrium with the jet, i.e., when there is no flow of heat between the jet and the heat transfer surface. The results also showed that the axial velocity and temperature profiles downstream of the potential core are very similar. It then follows that the radial profiles of adiabatic wall temperature could be collapsed onto a single curve using the following expression

$$(T_{aw} - T_{amb})/(T_n - T_{amb}) = f(x/x_{1/2})$$

where the jet half width, $x_{1/2}$, is the radius of the free jet at $U = U_m/2$ in the absence of the impingement plate.

At much larger temperature differences (typically up to 300°C) the density of the jet relative to that of the ambient air has a significant effect on the heat transfer coefficients and jet temperature dissipation. Katoaka (1985) correlated the potential core length, Pu, as a function of the Reynolds number and the density ratio.

$$Pu/D = 2.82(\rho_{amb}/\rho_n)^{-0.29}\mathrm{Re}^{0.07}$$

The potential core length reduces if the jet density is lower than the density of the ambient air. Katoaka also showed that the maximum stagnation point heat transfer occurs close to the

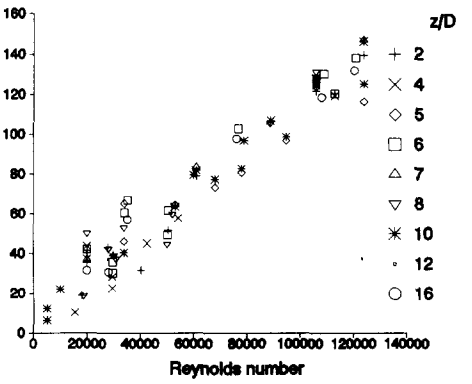

Figure 4 Local heat transfer ($\mathrm{Nu}/\mathrm{Pr}^{1/3}$) at $x/D = 6$ for z/D from 2–16

Table 1 Summary of sources of local heat transfer rates

Authors	Date	Nozzle geometry	Nozzle diameter (mm)	Re	z/D	Data	Other data	Measurement technique
Baughn and Shimizu	1989	Long pipe $l/D = 72$	25	23,750	2–14	Nu		Heated plate, liquid crystals
Baughn *et al.*	1991	Long pipe $l/D = 72$	25	23,300–55,000	2–10	Nu	Effectiveness	Heated plate, liquid crystals
Butler	1984	Contoured	12.7	61,000–124,000	2, 4, 6, 8, 10, 12	Nu	Recovery factor effectiveness	Heated plate
*Button and Wilcock	1982	Orifice $l/D = 0.25$	25.4	25,000	2–6	Nu	Velocity, turbulence	Naphthaline sublimation
Behbahani and Stewart	1989	Sharp orifice	6.35	4,800 10,000	15 10	Sh		Naphthaline sublimation
Chia	1972		32, 19	34,000	1.2–20	Sh	Turbulence, pressures	Naphthaline
Donaldson *et al.*	1971	Contoured	13	30,000–110,000	10–30	htc	Turbulence, pressure	Heat flux gauges
Den Ouden and Hoogendoorn	1974		13, 57	38,000–264,000	1–6	Nu	Turbulence	Heated plate, liquid crystals
*Gardon and Carbonpue	1962	Contoured low l/D	2.3–9	28,000	0.25–24	htc		Heat flux gauges
Gardon and Akfirat	1965	Contoured	0.25 in	2,500–28,000	2	htc	Turbulence	Heat flux gauges
*Goldstein and Behbahani	1982	Pipe $l/D = 7$	12.7	35,200–121,000	6	Nu	Recovery factor	Heated plate
		Orifice $l/D = 1$		35,100–120,500	12			
*Goldstein and Timmers	1982	Orifice $l/D = 1$	10	40,000	2, 6	Nu		Liquid crystals
Goldstein *et al.*	1986	ASME elliptical	12.7	61,000–124,000	2, 5, 8, 10	$Nu/Re^{0.7}$	Recovery factor	Heated plate
Goldstein and Franchett	1988	Orifice $l/D = 1$	10.0	10,000–30,000	4, 6, 10	Nu	Oblique impingement	Heated plate, liquid crystals
Goldstein *et al.*	1990	ASME elliptical	12.7	61,000–124,000	2–12	Nu	Recovery factor effectiveness	Heated plate
Gundappa *et al.*	1989	Pipe $l/D = 10$ Orifice	15.9 15.9	34,000	2.6, 5.2, 7.8	Nu		Heated plate
*Hollworth and Gero	1985	Orifice $l/D = 1$	2.5, 10	5,000–60,000	1, 5, 10, 15	$Nu/Pr^{0.3}$		Heat flux
*Hoogendoorn	1977	Contoured Pipe large l/D	57	66,000	2, 4, 5.9	Nu	Turbulence, pressure	Heated plate, liquid crystals
Katoaka *et al.*	1978	Contoured	28	4,000–15,000	2.5, 6, 8	mtc	Turbulence, velocities	Electro-Chemical
*Kieger	1981	Contoured	12.7	61,000–124,000	4, 5, 10	Nu	Recovery factor	Heated plate
*Lovell	1978	Sharp orifice	0.25 in	2,500–10,000	7, 10, 15	Nu	Impingement angle	Naphthaline sublimation
*Obot *et al.*	1979	Orifice and contoured pipes $l/D = 1$–50	19.05	15,000–54,000	2–12	Nu	Turbulence	Heated plate
*Obot *et al.*	1979	Contoured ASME	10, 20	18,000–52,000	4–24	Local and mean Nu	Turbulence	Heated plate
*Obot *et al.*	1982	Contoured ASME	20	18,000–50,100	2, 4, 6, 8	Nu		
*Popiel and Boguslawski	1988	Contoured and sharp orifice	14, 60 10, 15	4,590–63,100 5,940–44,220	1.2–16	Sh	Turbulence	Naphthaline sublimation
*Schlunder and Gnielinski	1967	Long pipe	20–50	34,000–124,000	1.25, 2.5, 5, 10	Sh		Water vaporization
*Sparrow and Lovell	1980	Sharp orifice	6.35	2,500–10,000	7, 10, 15	Nu	Effect impingement angle	Naphthaline sublimation

* Data used in the present study.

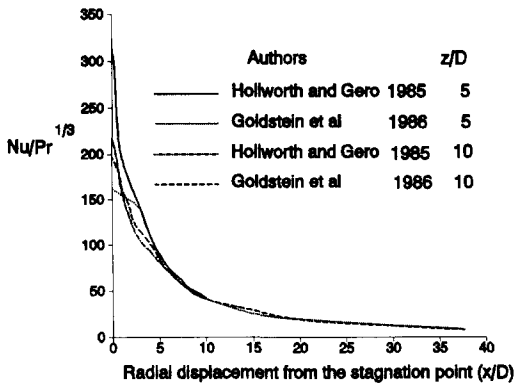

Figure 5 Heat transfer ($\overline{Nu}/Pr^{1/3}$) in the wall jet region based on Goldstein *et al.* (1986) and Hollworth and Gero (1985)

end of the potential core even though its length varies with density ratio.

The reduction of jet temperature due to mixing with the cooler ambient air should be taken into account when determining the adiabatic wall temperature and the heat flux.

A measure of the effect of temperature reduction due to mixing of a nonambient jet issuing from an orifice is given in Hollworth and Wilson (1984). The adiabatic wall temperature can be obtained from the following two correlations. The radial variation of local adiabatic wall temperature (T_{aw}) relative to the adiabatic wall temperature at the stagnation point ($T_{aw,s}$)

$$\alpha = (T_{aw} - T_{amb})/(T_{aw.s} - T_{amb})$$

and the axial variation of the stagnation point adiabatic wall temperature

$$\beta = (T_{aw.s} - T_{amb})/(T_n - T_{amb})$$

Goldstein and Behbahani (1982) expressed the effect of mixing between the jet and an ambient crossflow on the jet temperature in the form of

$$\text{Effectiveness} = (T_{aw} - T_{rec})/(T_{nozz} - T_{amb})$$

where

$$T_{rec} = t_n + R(T_n - t_n)$$

T_n and t_n are the jet total and static temperatures at the nozzle exit and T_{rec} is measured when $T_n = T_{amb}$. The recovery factor R is given by

$$R = (T_{aw} - t_n)/(U_n^2/2Cp)$$

Butler (1984) investigated the effectiveness and the recovery factor of a single circular jet issuing from an ASME nozzle in the absence of a cross flow. The results indicated that the effectiveness is dependent on z/D and x/D.

Figure 6 compares the jet effectiveness obtained by Butler with that derived from the product of α and β using the results of Hollworth and Wilson.

A correlation for effectiveness is given by Goldstein *et al.* (1990)

$$\text{Effectiveness} = 0.35 + 0.6e^{-0.01(z/D-2)^{2.2}-0.1(x/D)^{2.5}}$$

when $0 \leqslant x/D \leqslant 3.5$, and

$$\text{Effectiveness} = 1.193(x/D)^{-0.98}$$

when $x/D \geqslant 3.5$.

Baughn *et al.* (1991) compared the radial distribution of effectiveness obtained for an impinging jet issuing from a pipe with the distribution given by Goldstein *et al.* for an ASME elliptical nozzle. The results showed that, at all z/D tested, a jet issuing from the pipe has a greater effectiveness when $x/D \leqslant 3$. It has been shown by Tso and Hussain (1989) that vortices surrounding the jet enhance the mixing between the jet and the ambient air. The proposal of Popiel and Trass (1991) that a laminar layer (formed on the wall of a contoured convergent nozzle) between the jet and the ambient air causing the development of strong vortices might provide an explanation for the difference in behavior of the jets issuing from the two types of nozzles. This laminar layer would be thinner at the exit to a long pipe where the flow is fully developed than in an ASME elliptical nozzle, resulting in weaker vortices and so less mixing between the jet and the ambient air.

Butler (1984), Goldstein *et al.* (1990), and Baughn *et al.* (1991) all suggest that effectiveness is independent of nozzle exit Reynolds number.

Correlations for local heat transfer derived from published data

An analysis of the stagnating laminar flow on a cylinder by Sibulkin (1952) showed that the Nusselt number at the stagnation point is a function of Reynolds number to the power 0.5. Popiel and Boguslawski (1988) gave a correlation for the contoured ASME nozzle:

$$Sh_s = (0.508 + 0.051z/D)\,Re^{0.5}\,Sc^{0.4}$$

which applied in the range $1.2 \leqslant z/D \leqslant 5$. However, as the nozzle-to-plate spacing was increased to more than 7 nozzle diameters and the turbulent mixing zone penetrates to the jet axis the correlation reflects a turbulent flow. For $z/D \geqslant 7$

$$Sh_s = 0.461Re^{0.75}(z/D)^{-0.87}Sc^{0.4}$$

The form of the expression used by Hoogendoorn (1977) to correlate the stagnation point heat transfer has been used by a number of authors. Hoogendoorn gave the expression

$$\frac{Nu_s}{Re^{0.5}} = 0.65 + 2.03\left(\frac{Tu\,Re^{0.5}}{100}\right) - 2.46\left(\frac{Tu\,Re^{0.5}}{100}\right)^2$$

where $1 \leqslant z/D \leqslant 10$, Pr = 0.7, and Re and Tu (the turbulence intensity) are the values obtained from the free jet at an axial displacement from the nozzle equal to the nozzle-to-plate spacing. This expression shows that as the turbulence increases, the weight given to the exponents of Reynolds number greater than 0.5 also increases.

In the wall jet region ($x/D \geqslant 4.5$) experimental work (e.g., Rao and Trass 1964) shows that $Nu \propto Re^a$, where a is in the region of 0.8 for turbulent flows. A transition from laminar to

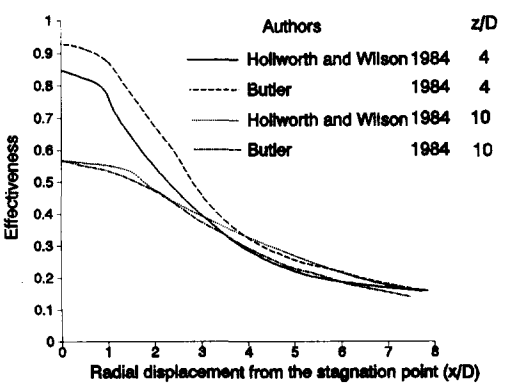

Figure 6 Jet effectiveness at $z/D = 4$ and 10. (From Hollworth and Wilson 1984, and Butler 1984)

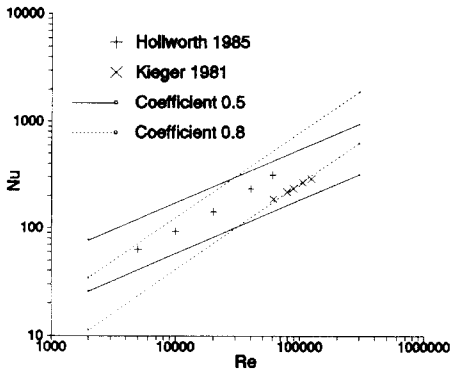

Figure 7 Local heat transfer at the stagnation point at $z/D = 5$

fully turbulent flow is expected to occur between the stagnation point and $x/D = 4.5$ at low nozzle-to-plate spacings. At higher nozzle-to-plate spacings the boundary layer at the stagnation point will be turbulent. This suggests that a correlation for local heat transfer coefficient should be in the form

$$Nu \propto Re^a$$

where $a = f(x/D, z/D)$.

Source of information

The review of the jet impingement literature (bibliographies are given in Button and Wilcock [1978] and Button and Jambunathan [1989]) yielded a number of publications giving local values for the heat transfer due to a single impinging circular jet. The data reported covers contoured nozzles, e.g. ASME elliptical type, square-edged orifices, sharp-edged orifices and long pipes. The sources considered in deriving the results presented here are indicated by an asterisk in Table 1. The heat transfer data was extracted by digitizing the graphs given in the publications using a digitizer that has a resolution of 0.1 mm. Small graphs were photographically enlarged; the resulting nonlinearities were less than 2 percent. Errors in the positioning of the digitizer cursor were estimated to be less than 0.5 mm. If a typical data point is assumed to be 100 mm from the axes, then the resulting position error is less than 0.5 percent. A combined error ($= \sqrt{(0.02^2 + 0.005^2)}$) of approximately 2.1 percent is incurred for the conversion of a typical data point from a graph to digital form.

Effect of Reynolds number

Plots of the experimental values of local Nu obtained at the stagnation point for $z/D = 5$ and 10 are given in Figures 7 and 8. These show considerable scatter in the experimental results from the various sources but suggest that the exponent of Re in the relationship

$$Nu \propto Re^a$$

will be approximately constant over a range of Reynolds numbers. Figure 9 shows the variation of the exponent with radial displacement from the stagnation point and with nozzle-to-plate spacing. Linear regression using the logarithms of Nusselt number and Reynolds number was used to obtain the exponent a in the relation $Nu \propto Ra^a$. The exponent was derived for values of x/D from 0–6 and for values of z/D between 1.2 and 10. Only data from single experiments where three or more data points were available were considered. Of this data the results from six sources have not been included in the derivation of the correlations. The data of Schlunder and Gnielinski (1967) gives a relationship for the stagnation point heat transfer where the exponent for Reynolds number is less than the laminar value of 0.5. The data from Obot *et al.* (1979b, 1979c, and 1982) are based on measurements of the temperature of a series of rings concentric with the stagnation point and varying in width from 1/3 to 1.5 nozzle diameters. The resulting radial distributions of Nusselt number showed a local minimum in the region of the stagnation point even at large nozzle-to-plate spacings. This phenomenon has not been observed in the results of other experiments, suggesting an error in the derivation of the Nusselt number distributions. The exponent of Reynolds number derived from the data of Goldstein and Behbahani (1982) varies only between 0.59 and 0.66 in the range $0 \leqslant x/D \leqslant 6$. It is not clear why this should be so as the apparatus used was similar to that used by Kieger (1981), whose data gives the expected variation in exponent. The results of Sparrow and Lovell (1980), which also show a low value for the exponent of Reynolds number at larger radial displacements from the stagnation point, were obtained at nozzle exit Reynolds numbers between 2,500 and 10,000. These Reynolds numbers are lower than the Reynolds numbers in the other data considered. The trend shown in Figure 9 is for the exponent at the stagnation point to increase from the laminar value of 0.5 as the nozzle-to-plate spacing is increased and for the exponent to increase as the radial displacement from the stagnation point is increased. An expression has been developed to reflect these trends. An expression of this form should be incorporated into a correlation for local heat transfer coefficients. If

$$Nu \propto Re^a$$

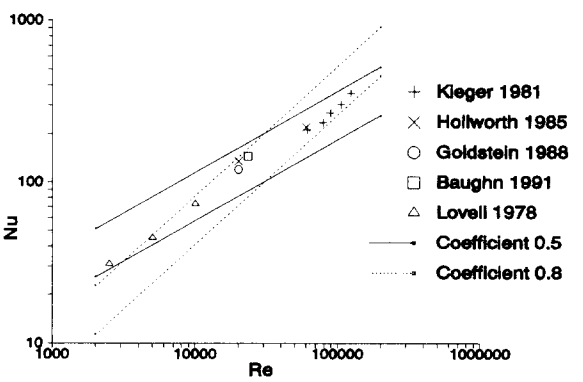

Figure 8 Local heat transfer at the stagnation point at $z/D = 10$

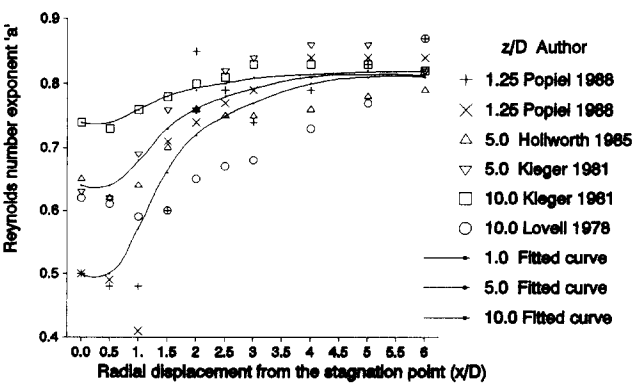

Figure 9 $Nu = f(Re^a)$, radial variation in the exponent a

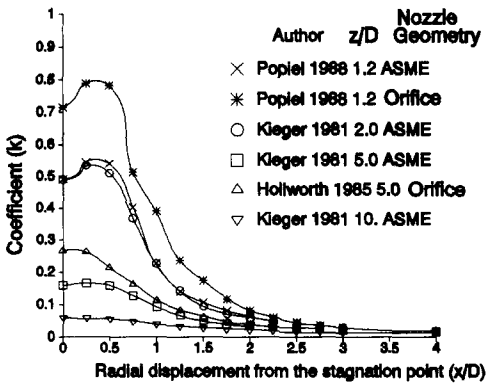

Figure 10 Heat transfer due to a single circular jet impinging on a flat plate

Table 2 Maximum uncertainties for the correlation coefficient

z/D	Nozzle geometry	x/D	95% Confidence interval (%)
1.2	Contoured	2.0	11
1.2	Orifice	1.0	25
2.0	Contoured	3.0	23
5.0	Orifice	0.0	4.1
5.0	Contoured	4.0	4.2
10.0	Contoured	0.0	4.1

then

$$a = 0.82 - \frac{0.32}{\left(1 + A\left(\frac{x}{D}\right)^k + B\left(\frac{x}{D}\right)^l\right)\left(1 + C\left(\frac{z}{D}\right)^m + D\left(\frac{z}{D}\right)^n\right)}$$

where $A = -1.95$, $B = 2.23$, $C = -0.21$, $D = 0.21$, $k = 1.8$, $l = 2$, $m = 1.25$, and $n = 1.5$.

If this assumption is made it is possible to develop a correlation for local Nusselt number in the form

$$Nu = f(Re^a, z/D, x/D)$$

where $a = f(x/D, z/D)$.

A curve of the form

$$Nu = kRe^a$$

where k is a constant and a is the function of x/D and z/D given above, was fitted through the results for 14 values of x/D between 0 and 4 for each of the values of z/D where sufficient data were available. This relationship assumes no heat transfer at zero nozzle flow, implying that the contribution of free convection is insignificant. This assumption is justified by the small temperature differences between the plate and the ambient air in the majority of the experiments on which this work is based.

The resulting curves of k or Nu/Re^a against x/D are plotted in Figure 10. The scatter of the data on which k is based varies with the radial displacement from the stagnation point. This results in a radial variation in the uncertainty of the values derived for k. Table 2 gives the 95 percent confidence interval for the value of k at the radial position where the scatter in the measured data is the greatest and hence where the confidence interval is also the largest. The confidence interval gives the range within which the fitted curve might be expected to fall, assuming that the scatter in the measured results is random.

The effect of nozzle-to-plate spacing and of radial displacement from the stagnation point

The curves shown in Figure 10 could be approximated by correlations of the form

$$\frac{Nu}{Re^a} = \frac{K}{1 - (x/D)^n}$$

where $1 \leqslant n \leqslant 2$, $a = f(x/D, z/D)$, and K is a constant. Since the curves are dissimilar, a different value of n would be required depending on the nozzle-to-plate spacing. Also there would be a considerable loss of accuracy in the region of the stagnation point where there is a local minimum in the value of k.

Discussion

Many papers are available that consider the effect of nozzle-to-plate spacing and Reynolds number on the Nusselt number. More recently the significance of other parameters such as nozzle geometry and confinement have been appreciated and investigations made into their effects. It appears that nozzle geometry affects the generation of turbulence in the shear layer. At nozzle-to-plate spacings of less than 10 diameters the use of an orifice will probably yield higher rates of heat transfer than a contoured nozzle. Other work suggests that the use of a pipe will also result in higher rates of heat transfer than a contoured nozzle at larger nozzle-to-plate spacings. A definitive statement on which nozzle geometry should be used to give the highest rates of heat transfer is probably not possible at present because this would involve a comparison between results from different experiments where factors apart from the nozzle geometry are significant. The optimal design of a jet impingement system is further complicated by the mixing of the ambient air with the jet. Where the temperature difference between the jet and the heat transfer surface is large compared with the temperature difference between the ambient air and the heat transfer surface, mixing will tend to reduce the exchange of energy between the jet and the heat transfer surface. The factors that cause an increase in turbulence, and so an increase in heat transfer rate, may also be expected to increase the dissipation of the jet temperature and so may in fact cause a reduction in the heat energy transferred.

The experimental data can be divided into three groups according to the type of jet nozzle used: ASME elliptic nozzles, orifices, and pipes. Figure 10 shows that the Nusselt number for an orifice jet is significantly greater than for an ASME elliptic nozzle. The effect of nozzle geometry is most significant at the stagnation point and is reduced as x/D increases. The effect of nozzle geometry is also greater at smaller nozzle-to-plate spacings.

Figures 7 and 8 show that $Nu \propto Re$ and suggest that at the stagnation point the exponent a is independent of Reynolds number in the range 5,000–124,000. Figure 9 shows that a is dependent on the radial displacement from the stagnation point and the nozzle-to-plate spacing. Previous correlations have either assumed that the exponent of Reynolds number is independent of both z/D and x/D or that the correlation applies to only a very limited range of values for z/D and x/D. For example, Goldstein and Franchett (1988) proposed a correlation,

$$Nu/Re^{0.7} = A\, e^{-(B + C\cos\phi)(x/D)^m}$$

where ϕ is the impingement angle, and gave different values for each of the coefficients for nozzle-to-plate spacings from 4–10 nozzle diameters. This correlation is based on data obtained for Reynolds numbers in the range $10{,}000 \leqslant Re \leqslant$

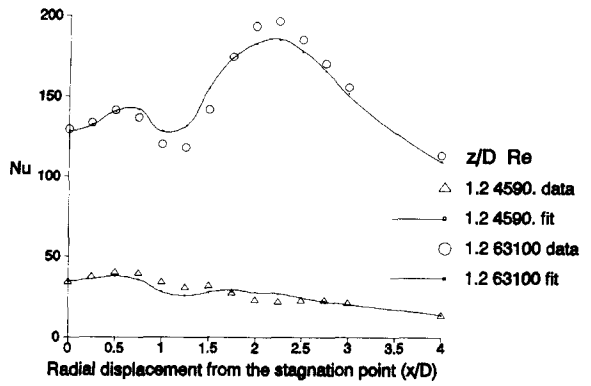

Figure 11 Radial variation in heat transfer between a plate and an impinging jet. Comparison of measurements and correlations. (Data obtained by Popiel and Boguslawski [1988] using an ASME nozzle)

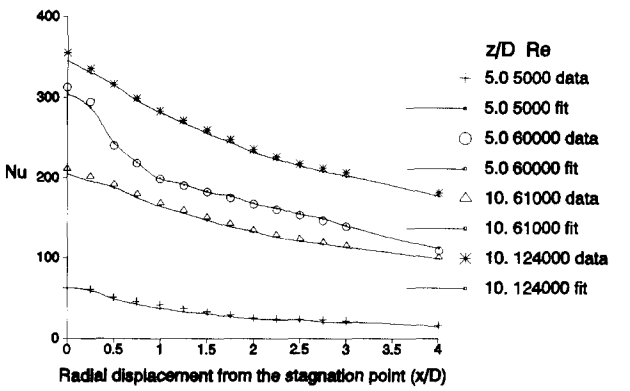

Figure 12 Radial variation in heat transfer between a plate and an impinging jet. Comparison of measured data and correlations. (Data from Hollworth and Gero [1985] obtained at $z/D = 5$ using an orifice and from Kieger [1981] obtained at $z/D = 10$ using an ASME nozzle)

30,000. A correlation in which the exponent of Reynolds number is given as a function of both x/D and z/D should be applicable over a wider range of parameter values without the need to change the correlation coefficients.

Figures 11 and 12 compare the radial distribution of Nu derived from the correlations with experimental values taken from the literature. These show a reasonable agreement between the correlations and experimental values.

Conclusions

A review of the empirical results confirms that the simplest correlations for local heat transfer coefficient should be of the form

$$\mathrm{Nu} = f(\mathrm{Re}, z/D, x/D, \mathrm{Pr})$$

but that these correlations will not account for the significant effects of nozzle geometry, confinement, and the generation of turbulence upstream of the jet nozzle. It has been demonstrated that the prediction of heat transfer also must include a consideration of the dissipation of jet temperature. This requires the use of local rather than area mean heat transfer coefficients.

The review clearly shows that details of the nozzle geometry, the confinement of flow, and the turbulence intensity at the nozzle exit are required if comparisons between different sets of experimental results are to be used to obtain an improvement in the understanding of the jet impingement heat transfer process.

Graphical correlations have been obtained for the local heat transfer due to a single impinging jet in the form

$$\frac{\mathrm{Nu}}{\mathrm{Re}^{f(x/D, z/D)}} = f_1(x/D, z/D)$$

where

$$f(x/D, z/D) = 0.82 - \frac{0.32}{\left(1 + \mathrm{A}\left(\frac{x}{D}\right)^{\mathrm{k}} + \mathrm{B}\left(\frac{x}{D}\right)^{\mathrm{l}}\right) \times \left(1 + \mathrm{C}\left(\frac{z}{D}\right)^{\mathrm{m}} + \mathrm{D}\left(\frac{z}{D}\right)^{\mathrm{n}}\right)}$$

and $\mathrm{A} = -1.95$, $\mathrm{B} = 2.23$, $\mathrm{C} = -0.21$, $\mathrm{D} = 0.21$, $\mathrm{k} = 1.8$, $\mathrm{l} = 2$, $\mathrm{m} = 1.25$, and $\mathrm{n} = 1.5$. This correlation is shown to be satisfactory at the nozzle-to-plate spacings for which heat transfer data are available over a range of Reynolds numbers. This correlation gives Nusselt number as a function of Reynolds number raised to an exponent where the exponent depends on the nozzle-to-plate spacing and the radial displacement from the stagnation point. A relationship of this form is suggested by the empirical data. It is suggested that future work in developing correlations when more data are available should follow a similar approach.

In conjunction with the results given by other authors, e.g., Goldstein *et al.* (1990), who investigated the dissipation of a nonambient jet, the correlations can be used to derive the heat transfer to a plate when the air temperature at the nozzle exit is not equal to the ambient temperature.

Jets issuing from square-edged orifices give higher heat transfer than jets from ASME elliptical nozzles.

The data considered in this review support the suggestion that the heat transfer coefficients in the wall jet are independent of nozzle-to-nozzle spacing z/D in the range of 1–12 nozzle diameters. Approximate values of heat transfer coefficient in the wall jet can be obtained by the extrapolation of the local value at $x/D \geqslant 4.5$ using the relationship

$$\mathrm{Nu} \propto (x/D)^{-1}$$

Acknowledgment

The post held by M. A. Moss is funded by the Polytechnics and Colleges Funding Council (PCFC) under their special research initiative and is gratefully acknowledged. The authors also wish to thank D. Corlett for her work in maintaining the collection of jet impingement literature on which this work is based.

References

Baughn, J. W., Hechanova, A. E. and Xiaojun, Y. 1991. An experimental study of entrainment effects on the heat transfer from a flat surface to a heated circular impinging jet. *Proc. of the ASME/JSME Joint Conf. Thermal Engineering*, Reno, NV, USA, March 17–22

Baughn, J. W. and Shimizu, S. 1989. Heat transfer measurements from a surface with uniform heat flux and an impinging jet. *J. Heat Transfer Trans. ASME*, **111**, 1096–1098

Behbahani, A. I. and Stewart, B. W. 1989. Measurement of the local mass transfer coefficient by holographic interferometry. *National Heat Transfer Conf. HTD*, **112**

Butler, K. A. 1984. Effect of entrainment on the heat transfer

between a flat surface and impinging circular air jets. M.Sc. thesis, University of Minnesota, MN, USA

Button, B. L. and Jambunathan, K. 1989. Jet impingement heat transfer: a bibliography 1976–1985. *Previews Heat Mass Transfer*, **15**, 149–178

Button, B. L. and Wilcock, D. 1978. Impingement heat transfer—a bibliography 1890–1975. *Previews Heat Mass Transfer*, **4**, 83–89

Button, B. L. and Wilcock, D. 1982. Effect of nozzle geometry on circular jet impingement heat transfer. *2nd Polytechnic Symposium on Thermodynamics and Heat Transfer*, Leicester, UK, November 16–17, 86–99

Chia, C. J. 1972. Mass transfer in an impinging jet. Ph.D. thesis, University of Toronto, Ontario, Canada

Dawson, D. A. and Trass, O. 1966. Mass transfer in a turbulent radial wall jet. *Canadian J. of Chemical Engineering*, **V44**, 121–129

Den Ouden, C. and Hoogendoorn, C. J. 1974. Local convective-heat-transfer coefficients for jets impinging on a plate: experiments using a liquid-crystal technique. *Proc. 5th Int. Heat Transfer Conf.*, Tokyo, Japan, September 3–7, **5**, 293–297

Donaldson, C. DuP., Snedeker, R. S. and Margolis, D. P. 1971. A study of free jet impingement. Part 2. Free jet turbulent structure and impingement heat transfer. *J. Fluid Mech.*, **45**, 477–512

Gardon, R. and Akfirat, J. C. 1965. The role of turbulence in determining the heat-transfer characteristics of impinging jets. *Int. J. Heat Mass Transfer*, **8**, 1261–1272

Gardon, R. and Carbonpue, J. 1962. Heat transfer between a flat plate and jets of air impinging on it. *Int. Developments in Heat Transfer, Int. Heat Transfer Conf.*, University of Colorado, CO, USA, August 28 to September 1, **2**, 454–460

Gauntner, J. W., Livingood, J. N. B. and Hrycak, P. 1970. Survey of literature on flow characteristics of a single turbulent jet impinging on a flat plate. *NASA* TN D-5652 NTIS N70-18963

Giralt, F., Chia, C. J. and Trass, O. 1977. Characterization of the impingement region in an axisymmetric turbulent jet. *Ind. Eng. Chem. Fundam.*, **16**, 21–28

Goldstein, R. J. and Behbahani, A. I. 1982. Impingement of a circular jet with and without crossflow. *Int. J. Heat Mass Transfer*, **25**, 1377–1382

Goldstein, R. J., Behbahani, A. I. and Kieger Heppelmann, K. 1986. Streamwise distribution of the recovery factor and the local heat transfer coefficient to an impinging circular air jet. *Int. J. Heat Mass Transfer*, **29**, 1227–1235

Goldstein, R. J. and Franchett, M. E. 1988. Heat transfer from a flat surface to an oblique impinging jet. *ASME J. Heat Transfer*, **110**, 87–93

Goldstein, R. J., Sobolik, K. A. and Seol, W. S. 1990. Effect of entrainment on the heat transfer to a heated circular air jet impinging on a flat surface. *ASME J. Heat Transfer*, **112**, 608–611

Goldstein, R. J. and Timmers, J. F. 1982. Visualization of heat transfer from arrays of impinging jets. *Int. J. Heat Mass Transfer*, **25**, 1377–1382

Gundappa, M., Hudson, J. F. and Diller, T. E. 1989. Jet impingement heat transfer from jet tubes and orifices. *National Heat Transfer Conf.*, Philadelphia, PA, USA, August 6–9, **107**, 43–50

Hollworth, B. R. and Gero, L. R. 1985. Entrainment effects on impingement heat transfer. Part 2. Local heat transfer measurements. *J. Heat Transfer Trans. ASME*, **107**, 910–915

Hollworth, B. R. and Wilson, S. I. 1984. Entrainment effects on impingement heat transfer. Part 1. Measurements of heated jet velocity and temperature distributions and recovery temperatures on target surface. *J. Heat Transfer. Trans. ASME*, **106**, 797–803

Hoogendoorn, C. J. 1977. The effect of turbulence on heat transfer at a stagnation point. *Int. J. Heat Mass Transfer*, **20**, 1333–1338

Hrycak, P. 1978. Heat transfer from a row of jets impinging on concave semi-cylindrical surface. *Proc. 6th Int. Heat Transfer Conf.*, Toronto, Ontario, Canada, August 2, 67–72

Katoaka, K. 1985. Optimal nozzle-to-plate spacing for convective heat transfer in nonisothermal, variable density impinging jets. *Drying Technol.*, **3**, 235–254

Kataoka, K., Harada, T. and Sahara, R. 1988. Mechanism for enhancement of heat transfer in turbulent impinging jets. *Current Research in Heat and Mass Transfer: A Compendium and a Festschrift for Professor Arcot Ramachandran* (M. V. Krishna Murthy *et al.*, Eds.), Hemisphere, New York

Katoaka, K., Komai, T. and Nakamura, G. 1978. Enhancement mechanism of mass transfer in a turbulent impinging jet for high Schmidt numbers. *ASME* Paper 78-HT-5

Kataoka, K., Suguro, M., Degawa, H., Maruo, K. and Mihata, I. 1987. The effect of surface renewal due to large-scale eddies on jet impingement heat transfer. *Int. J. Mass Transfer*, **30**, 559–567

Kieger, K. K. 1981. Local and average heat transfer from a flat surface to a single circular jet of air impinging on it. M.Sc. thesis, University of Minnesota, MN, USA

Launder, B. E. 1991. Private communication, October 10

Lepicovsky, J. 1989. The role of nozzle-exit boundary layer velocity gradient in mixing enhancement of free jets. *Proc. 3rd Joint ASCE/ASME Mechanics Conf.*, San Diego, CA, USA, July 9–12

Lovell, B. J. 1978. Local transfer coefficients for impingement of an axisymmetric jet on an inclined flat plate. M.Sc. thesis, University of Minnesota, MN, USA

Martin, H. 1977. Heat and mass transfer between impinging gas jets and solid surfaces. *Advances in Heat Transfer*, **13**, 1–60

Mitachi, K. and Ishiguro, R. 1977. Heat transfer of radial wall jets. Second report; Measurements of temperature field and heat transfer for radial wall jet. *Heat Transfer-Japan Res.*, **6**, 55–65

Obot, N. T., Mujumdar, A. S. and Douglas, W. J. M. 1979a. Design correlations for heat and mass transfer under various turbulent impinging jet configurations. *Developments in Drying*, 388–402

Obot, N. T., Mujumdar, A. S. and Douglas, W. J. M. 1979b. Effect of nozzle geometry on impingement heat transfer under a round turbulent jet. *ASME* Paper 79-WA/HF-53

Obot, N. T., Mujumdar, A. S. and Douglas, W. J. M. 1979c. Heat transfer under axisymmetric turbulent impinging jets. *AIChE 72nd Ann. Conf.*, San Francisco, CA, USA, A1-C3

Obot, N. Y., Mujumdar, A. S. and Douglas, W. J. M. 1982. Effect of semi-confinement on impingement heat transfer. *Proc. 7th Int. Heat Transfer Conf.*, Munchen, Germany, September 6–10, **3**, 395–400

Popiel, C. O. and Boguslawski, L. 1988. Effect of flow structure on the heat or mass transfer on a flat plate in impinging round jet. *2nd UK National Conf. on Heat Transfer*, University of Strathclyde, UK, September 14–16, **1**, 663–685

Popiel, C. O. and Trass, O. 1982. The effect of ordered structure of turbulence on momentum, heat, and mass transfer of impinging round jets. *Proc. 7th Int. Heat Transfer Conf.*, Munchen, Germany, September 6–10, **6**, 141–146

Popiel, C. O. and Trass, O. 1991. Visualization of a free and impinging round jet. *Exp. Thermal Fluid Sci.*, **4**, 253–264

Poreh, M., Tsuei, Y. G. and Cermak, J. E. 1967. Investigation of a turbulent radial wall jet. *J. Appl. Mech. Trans. ASME*, **34**, 457–463

Rao, V. V. and Trass, O. 1964. Mass transfer from a flat surface to an impinging turbulent jet. *Can. J. Chem. Eng.*, **42**, 95–99

Schlichting, H. 1968. *Boundary-Layer Theory*. McGraw-Hill, New York, 681

Schlunder, E. U. and Gnielinski, V. 1967. Heat and mass transfer between surfaces and impinging jets. *Chem. Ing. Tech.*, **39**, 578–584 (Translation held by BLDSC)

Sibulkin, M. 1952. Heat transfer near the forward stagnation point of a body of revolution. *J. Aeronautical Sci.*, August

Sparrow, E. M. and Lovell, B. J. 1980. Heat transfer characteristics of an obliquely impinging circular jet. *J. Heat Transfer. Trans. ASME*, **102**, 202–209

Tani, I. and Komatsu, Y. 1966. Impingement of a round jet on a flat surface. *Proc. of the Eleventh International Congress of Applied Mechanics* (H. Gortler, Ed.), Springer-Verlag, New York, 672–676

Tso, J. and Hussain, F. 1989. Organized motions in a fully developed turbulent axisymmetric jet. *J. Fluid Mech.*, **203**, 425–448

Welty, J. R., Wicks, C. E. and Wilson, R. E. 1976. *Fundamentals of Momentum, Heat and Mass Transfer*. Wiley, New York, 376–380

Yokobori, S., Kasagi, N., Hirata, M., Nakamaru, M. and Haramura, Y. 1979. Characteristic behavior of turbulence and transport phenomena at the stagnation region of an axi-symmetrical impinging jet. *Proc. 2nd Symp. Turb. Shear Flows*, London, UK, **4**, 4.12–4.17